OPTIMAL AEROASSISTED ORBITAL TRANSFER WITH PLANE CHANGE USING COLLOCATION AND NONLINEAR PROGRAMMING+

By

Yun. Y. Shi*, R. L. Nelson**, and D. H. Young***

McDonnell Douglas Space Systems Company
5301 Bolsa Avenue
Huntington Beach, California 92647

ABSTRACT

The fuel optimal control problem arising in the non-planar orbital transfer employing aeroassisted tehnology is addressesd. The mission involves the transfer from high energy orbit (HEO) to low energy orbit (LEO) with orbital plane change. The basic strategy here is to employ a combination of propulsive maneuvers in space and aerodynamic maneuvers in the atmosphere. The basic sequence of events for the aeroassisted HEO to LEO transfer consists of three phases. In the first phase, the orbital transfer begins with a deorbit impulse at HEO which injects the vehicle into an elliptic transfer orbit with perigee inside the atmosphere. In the second phase, the vehicle is optimally controlled by lift and bank angle modulations to perform the deisred orbital plane change and to satisfy heating constraints. Because of the energy loss during the turn, an impulse is required to initiate the third phase to boost the vehicle back to the desired LEO orbital altitude. The third impulse is then used to circularize the orbit at LEO. The problem is solved by a direct optimization technique which uses piecewise polynomial representation for the state and control variables and collocation to satisfy the differential equations. This technique converts the optimal control problem into a nonlinear programming problem which is solved numerically. Solutions were obtained for cases with and without heat constraints and for cases of different orbital inclination changes. The method appears to be more powerful and robust than other optimization methods. In addition, the method can handle complex dynamical constraints.

---

* Staff Manager, ** Principal Scientist, *** Manager, Flight Mechanics/Advanced Systems Analysis

+ The senior author wishes to thank Professor P.E.Gill for helpful discussions on the structure of the nonlinear programming codes, i.e., NZSOL and NPSOL. He also wishes to thank Greg Badum for computing supports and graphics.

NOMENCLATURE

A	:	$S\rho_s/2$
C_D	:	drag coefficient
C_{DO}	:	zero-lift drag coefficient
C_L	:	lift coefficient
C_{LR}	:	lift coefficient for maximum lift-to-drag rati
D	:	drag force
g	:	gravitational acceleration
g_s	:	gravitational acceleration at surface level
H	:	altitude
J	:	performance index
K	:	induced drag factor
L	:	lift force
m	:	vehicle mass
R	:	distance from Earth center to vehicle center of gravity
R_a	:	radius of the atmospheric boundary
R_c	:	radius of the low Earth orbit (LEO)
R_d	:	radius of the high Earth orbit (HEO)
R_E	:	radius of Earth
S	:	aerodynamic reference area
t	:	time
V	:	velocity
T	:	Thrust
β	:	inverse atmospheric scale height
γ	:	flight path angle
ψ	:	heading angle
σ	:	bank angle
θ	:	down range angle or longitude
ϕ	:	cross range angle or latitude
μ	:	gravitational constant of Earth
ρ	:	density
ΔV	:	characteristic velocity

subscripts

c	:	subscript for circularization or reorbit
d	:	subscript for deorbit
s	:	subscript for surface level

1. INTRODUCTION

In order to have a viable and affordable space program, advanced technology must be exploited and new design concepts must be developed to reduce the size and cost of transportation elements for supporting new mission requirements. One of the new concepts that has evolved in recent years to advance the cost effectiveness of space transportation systems is the aerodynamically assisted orbit transfer. Such an orbital transfer vehicle is designed with an aerodynamic configuration which can utilize the planetary atmosphere for the purpose of energy management. Numerous studies have demonstrated that the use of the aerobraking can significantly reduce the

propulsive velocity requirements for certain class of orbit transfers. Excellent review papers were given by Warberg (Reference 1) and Mease (Reference 10).

In this paper, the fuel optimal control problem arising in a typical orbit transfer with plane change from HEO to LEO as discussed in most recent publications is addressed. In this case, as discussed in Reference 2, the aeroassisted orbit transfer vehicle (AOTV) maneuver involves three propulsive burns or impulses as sketched in Fig.1. In the first phase , the transfer begins with a deorbit impulse at HEO which injects the vehicle into an elliptic transfer orbit with the perigee inside the atmosphere. In the second phase, the vehicle is inside the atmosphere and is optimally controlled by the lift and bank angle modulations to perform the desired orbital plane change and to satisfy the heating rate and other physical constraints. Because of the the energy loss during the atmospheric maneuvers, an impulse is required to initiate the third phase to boost the vehicle back to the final orbital altitude. Finally, the third impulse is applied to circularize the orbit at LEO. In summary, there are three propulsive burns and an aeroassist plane change inside the atmosphere. Simulation results similar to those obtained in the draft paper of Reference 2 have been obtained here by using the Hermite polynomial and collocation technique to convert the optimal control problem into a nonlinear programming (NP) problem which is solved numerically using the optimization code, NZSOL (cf. Reference 12) provided by Gill, which is an improved version of NPSOL (cf. Reference 6), developed at Stanford. This solution method is different from the indirect method such as those discussed in Reference 2,4,7 and 8. The above simulation results have been extended to cases with heating constraints and cases for different orbit inclination changes. The details are presented and discussed in this paper. It is important that in the future these simulations be extended to include all other realistic flight constraints and to establish baseline optimum trajectory characteristics for GEO to Space station or shuttle, lunar and Mars missions.

2. DIRECT TRAJECTORY OPTIMIZATION WITH COLLOCATION AND HERMITE POLYNOMIALS

In the direct collocation with nonlinear programming approach, the trajectory is approximated by piecewise polynomials, which represent the state and control variables at a number of discrete time points, i.e., nodes. For a given state variable, the state trajectory over a given "segment" between two nodes is taken to be the unique Hermite cubic which goes through the end points of the segments with the appropriate derivatives that are dictated by the differential equations of motion at the endpoints. This is the "Hermite cubic" since it is determined by the states and their derivatives. A collocation is taken at the center of the segment where the derivative given by the Hermite cubic is compared to the derivative obtained from the evaluation of the equations of motion. The difference is termed the "defect" and is a measure of how well the equations of motion are satisfied over the segments. If all the defects are zero, then the differential equations are satisfied at the center collocation points as well as at the endpoints. Figure 2 shows the typical defects between node 1 and node 2.

Let the system of equations of motion be given as

$$X' = f(X,U) \tag{2-1a}$$

where X is the state vector and U is the control vector and (') denotes the differentiation with respect to the time. Let the time over a given segment be T. For the problem discussed here, one can show that

$$X = (x, y, z, x', y', z', m)$$
$$U = (C_L, \sigma) \tag{2–1b}$$

Then the Hermite interpolated x-component of the state vector X at the center point is

$$x_c = (1/2)\,(x_1 + x_r) + (T/8)\,[f(X_1,U_1) - f(X_r,U_r)] \tag{2-2}$$

where x_1 and x_r are respectively the x-component of the state vector X at the left and the right nodes. The derivative of the interpolating Hermite cubic at the center point is

$$x_c' = -3/(2T)\,(x_1 - x_r) - (1/4)\,[f(X_1,U_1) + f(X_r,U_r)] \tag{2-3}$$

The defect vector is then calculated as

$$d = f(X_c,U_c) - x_c' \tag{2-4}$$

If x_1, u_1, x_r, and u_r are chosen such that the elements of the defect vector, d, are sufficiently small, the "Hermite polynomials" become an accurate approximation to the solution of the differential equations of motion (by implicit integration). With the above approach, the differential equations are converted into nonlinear algebraic equations and the optimal control problem can then be solved using the nonlinear programming techques.

3. APPLICATION TO OPTIMAL AEROASSISTED ORBITAL TRANSFER WITH PLANE CHANGE

The aeroassited orbital transfer can be analyzed in three phases , i.e., deorbit, aeroassist (or atmospheric flight), boost and reorbit (or circularization). In each of the phases, a particular set of equations of motion apply.

3.1 Deorbit

Initially, the spacecraft is moving with a circular velocity $V_d = \sqrt{\mu / R_d}$ in a circular orbit of radius R_d, well outside the Earth's atmosphere. Deorbit is accomplished at point D by means of an impulse ΔV_d, to transfer the vehicle from a circular orbit to an elliptic orbit with perigee low enough for the trajectory to intersect the dense part of the atmosphere. Since the elliptic velocity at D is less than the circular velocity at D, the impulse ΔV_d is executed so as to oppose the circular Velocity V_d. In other words, at point D, the velocity required to put the vehicle into elliptic orbit is less than the velocity required to maintain it in circular orbit. The deorbit impulse ΔV_d causes the vehicle to

enter the atmosphere at radius R_a with a velocity V_e and flight path angle γ_e. It is known that the optimal energy loss maneuver from the circular orbit is simply the Hohmann transfer and the impulse is parallel and opposite to the instantaneous velocity vector.

After applying the deorbit impulse and before entering the atmosphere at R_a, the deorbit trajectory is a coasting arc and known integrals of the equations of motion can be used to relate the state vectors at R_a, the entry into atmosphere to the state vectors right after the deorbit impulse at R_d. Using the principle of conservation of energy and angular momentum at the deorbit point D and the atmospheric entry point E, we get

$$V_e^2/2-\mu/R_a=(V_d-\Delta V_d)^2/2-\mu/R_d \tag{3-1}$$

$$R_a V_e \cos(-\gamma_e)=R_d(V_d-\Delta V_d) \tag{3-2}$$

from which we can solve for ΔV_d to get

$$\Delta V_d=\sqrt{\mu/R_d}-\sqrt{2\mu(1/R_a-1/R_d)/\left[(R_d/R_a)^2/\cos^2\gamma_e-1\right]} \tag{3-3}$$

It is easily seen that the minimum deorbit impulse ΔV_{dm} obtained for $\gamma_e = 0$, corresponds to an ideal transfer with the space vehicle grazing the atmospheric boundary. To ensure proper atmospheric entry, the deorbit impulse ΔV_d must be higher than the following minimum deorbit impulse ΔV_{dm}

$$\Delta V_{dm}=\sqrt{\mu/R_d}-\sqrt{2\mu(1/R_a-1/R_d)/\left[(R_d/R_a)^2-1\right]} \tag{3-4}$$

Physically, the second term of the above equation corresponds to the apogee velocity of an ellpitic transfer orbit with perigee radius R_a and apogee radius R_d. This elliptic transfer orbit is tangent to the atmosphere boundary at perigee. It will be shown later that the nonlinear constraint equations (3-15) at the atmospheric entry point can also be derived from equations (3-1 and 2).

3.2 Aeroassist

During the atmospheric flight, the vehicle is optimally controlled by the lift and bank angle modulations to achieve the necessary velocity reduction (due to the atmospheric drag) and the plane change. In the present formulation, only the aeroassisted atmospheric flight need be solved by using the collocation and nonlinear programming techniques discussed earlier in this paper. The solutions in the other phases are provided by the known integral relations of the equations of motion because these arcs are coasting arcs.

Consider a vehicle with the point mass m, moving about a rotating spherical planet. The atmosphere surrounding the planet is assumed to be at rest, and the central gravitational field obeys the usual inverse square law. The equations of motion for the vehicle are given by (Figure 1),

$$\dot{r} = V \sin\gamma \tag{3-5a}$$

$$\dot{\theta} = \frac{V \cos\gamma \cos\psi}{r \cos\phi} \tag{3-5b}$$

$$\dot{\phi} = \frac{V \cos\gamma \sin\psi}{r} \tag{3-5c}$$

$$\dot{v} = \frac{(\eta T \cos\varepsilon - D)}{m} - \frac{\mu \sin\gamma}{r^2} + \omega^2 r \cos\phi (\sin\gamma \cos\phi - \cos\gamma \sin\psi \sin\phi) \tag{3-5d}$$

$$\dot{\gamma} = \frac{(\eta T \sin\varepsilon + L)\cos\sigma}{mV} - \frac{\mu \cos\gamma}{Vr^2} + \frac{V \cos\gamma}{r} + 2\omega \cos\psi \cos\phi$$

$$+ \frac{\omega^2 r \cos\phi}{V}(\cos\gamma \cos\phi + \sin\gamma \sin\psi \sin\phi) \tag{3-5e}$$

$$\dot{\psi} = \frac{(\eta T \sin\varepsilon + L)\sin\sigma}{mV \cos\gamma} - \frac{V \cos\gamma \cos\psi \tan\phi}{r} + 2\omega(\tan\gamma \sin\psi \cos\phi - \sin\phi)$$

$$+ \frac{\omega^2 r \cos\psi \sin\phi \cos\phi}{V \cos\gamma} \tag{3-5f}$$

$$\dot{m} = -f(r, V, \eta) \tag{3-5g}$$

where for a given vehicle, the drag D and the lift L are

$$D = \frac{S}{2m} \rho V^2 C_D \tag{3-5h}$$

$$L = \frac{S}{2m} \rho V^2 C_L \tag{3-5i}$$

and the drag and lift coefficients obey the drag-polar relation

$$C_D = C_{DO} + K C_L^2 \tag{3-5j}$$

Also, for an exponential atmosphere, one has

$$\rho = \rho_s \exp(-H\beta) \quad \text{and} \quad H = R - R_E \tag{3-5k}$$

Simulation results obtained here were using the U.S. standard Atmosphere 1976.

For the problem considered here, one assumes that, inside the atmosphere, the vehicle is optimally controlled by the aerodynamic forces only. Thus it is assumed that the thrust T is absent and the point mass is constant in this region. Furthermore, no earth rotation was assumed. The later is equivalent to consider the motion with respect to an earth fixed inertial coordinate system (ECI). The plane change or the orbit inclination, i, is related to the cross range ϕ and the heading angle ψ as

$$\cos i = \cos\phi \cos\psi \qquad t_e \le t \le t_f \tag{3-6}$$

The orbit inclination changes throughout the atmospheric flight and must end up with the required value at exit. For small values of cross range angle ϕ, i is given by the heading angle ψ itself.

3.3 Boost and Reorbit

During the atmospheric flight, the vehicle undergoes the plane change using the lift and bank angle modulation . Because of the loss of energy during the atmospheric maneuver, a second impulse is required at the exit from the atmosphere to boost the vehicle back to the final orbital altitude at LEO.

The vehicle exits the atmosphere at point F, with a velocity V_f and the flight path angle γ_f. The additional impulse ΔV_b, required at the exit point F for boosting the vehicle into an elliptic transfer orbit with apogee radius R_c, and the reorbit (or circularization) impulse ΔV_c, required to insert the vehicle into a circular orbit, are obtained by using the principle of conservation of energy and angular momentum at the exit point F and the reorbit or circularization point C. Thus, we have

$$(V_f + \Delta V_b)^2 / 2 - \mu / R_a = (V_c - \Delta V_c)^2 / 2 - \mu / R_c \tag{3-7}$$

$$(V_f + \Delta V_b) R_a \cos\gamma_f = R_c (V_c - \Delta V_c) \tag{3-8}$$

Solving for ΔV_b and ΔV_c from the above equations (3-7) and (3-8) yields

$$\Delta V_b = \sqrt{2\mu(1/R_a - 1/R_c) / \left[1 - (R_a/R_c)^2 \cos^2\gamma_f\right]} - V_f \tag{3-9}$$

$$\Delta V_c = \sqrt{\mu / R_c} - \sqrt{2\mu(1/R_a - 1/R_c) / \left[(R_c/R_a)^2 / \cos^2\gamma_f - 1\right]} \tag{3-10}$$

It is interesting to note that the second term of equation (3-10) is maximum for $\gamma_f = 0$ and therefore the reorbit impulse ΔV_c ,is minimum for $\gamma_f = 0$. It will be shown later that boundary conditions and nonlinear constraint equations at the exit point F, can be derived in terms of the final orbit characteristics and the final state vectors at the exit as shown in (3-16,17,& 18).

3.4 Performance Index

It is known that the change in speed, ΔV, also called the characteristic velocity, is a convenient parameter to measure the fuel consumption. For minimum-fuel maneuver, the objective is then to minimize the total characteristic velocities. A convenient performance index is the sum of the characteristic velocities for deorbit, boost, and reorbit, as

$$J = \Delta V_d + \Delta V_b + \Delta V_c \tag{3-11}$$

Where, ΔV_d, ΔV_b, and ΔV_c are the deorbit, boost, and reorbit characteristic velocities respectively, and are related as

$$\Delta V_d = \sqrt{\mu / R_d} - (R_a / R_d) V_e \cos(-\gamma_e) \tag{3-12}$$

$$\Delta V_c = \sqrt{\mu / R_c} - (R_a / R_c)(V_f + \Delta V_b)\cos\gamma_f \tag{3-13}$$

Alternatively, ΔV_d, ΔV_b, and ΔV_c are also given by (3-3, 9, and 10) respectively. Note that for a given final circular orbit, the impulses ΔV_b and ΔV_c are completely determined by the state variables V_f and γ_f at the exit of the atmospheric portion of the trajectory. The velocity V_e and the flight path angle γ_e at the atmospheric entry point are dependent only on the magnitude of the deorbit impulse ΔV_d. It follows that the optimal control problem needs to consider only the trajectory segment within the atmosphere subject to the nonlinear constraints and boundary conditions at the atmospheric entry and exit points. In addition, other path constraints such as the peak heating rate have to be satisfied.

3.5 Boundary conditions and constraints

The boundary conditions and constraints for the optimal control problem can be summarized as follows:

- At the entry into atmosphere, the following initial constraints.must be satisfied.

$$R = R_a \;;\; \gamma_e \le 0 \quad , \qquad \phi_e = 0, \;\; \psi_e = 0 \tag{3-14}$$

$$\frac{V_e^2}{2}\left[1 - \left(\frac{R_a}{R_d}\right)^2 \cos^2(\gamma_e)\right] - \mu\left(\frac{1}{R_a} - \frac{1}{R_d}\right) = 0 \tag{3-15}$$

The first initial constraint is required to ensure the vehicle enters the atmosphere. In the present formulation, the initial velocity and the flight path angle are unknown and to be determined by the optimization processes subject to the second constraint.

- At the exit from atmosphere, the following constraints must be satisfied.

$$R = R_a \;;\; \gamma_f \ge 0 \tag{3-16}$$

$$\frac{(V_f + \Delta V_b)^2}{2}\left(1 - \frac{R_a^2}{R_c^2}\cos^2\gamma_f\right) - \mu\left(\frac{1}{R_a} - \frac{1}{R_c}\right) = 0 \tag{3-17}$$

$$\cos i_f - \cos\phi_f \cos\psi_f = 0 \tag{3-18}$$

Equation (3-16) is required to ensure the vehicle exit the atmophere. The second costraint can be used to compute ΔV_b, and if ΔV_b,is assumed to be zero as in the case of aerobraking without orbit plane change, the above constraint must be imposed to determine the correct V_f and γ_f. The third constraint is required to perform the desired orbital plane change.

- In addition, there are other path constraints ,i.e., constraints must be satisfied along the trajectory such as
  - a) Stagnation Point Heating Rate Constraints
  - b) Altitude Constraints
  - c) Bounds on the Control Variables
  - d) Others

4. STRUCTURE AND SOLUTION OF THE NONLINEAR PROGRAMMING PROBLEM

The direct collocation and Hermite polynomial procedures described above convert optimal control problems into corresponding nonlinear programming problems. Ordinary differential equations are converted into corresponding nonlinear algebraic equations (or nonlinear "defects" constraint equations). These problems can then be solved using nonlinear programming codes.

The variables for the nonlinear programming problem are the collected state vectors and control vectors at the nodes and the time duration of phases. These quantities are assembled into the NLP state vectors

$$X^T = \left[X_1^T, U_1^T, \cdots\cdots X_n^T, U_n^T, t_1, t_2 \cdots\cdots t_k\right] \tag{4-1}$$

where n is the number of nodes and k is the number of phases on the trajectory. The defects and other physical and mathematical constraints are collected into the NLP constraint vector C

$$C^T = \left[d_1^T, d_2^T, \cdots\cdots d_n^T, w_1^T, w_2^T, w_3^T, \cdots\cdots w_j^T\right] \tag{4-2}$$

where d_i is the defect vector and w is a vector of additional problem constraints.

The nonlinear programming code used here is the NZSOL (Reference 12). The NZSOL is an improved version of the NPSOL (Reference 6) , developed by the Stanford Optimization Laboratory and designed to minimize a smooth nonlinear function subject to a set of constraints which may include simple bounds on the

variables, linear constraints, and smooth nonlinear constraints The problem is assumed to be stated in the following form:

NP

$$\underset{x \in R^n}{\text{minimize}} \quad F(x)$$

$$\text{subject to} \quad \ell \le \begin{Bmatrix} x \\ A_L x \\ c(x) \end{Bmatrix} \le u, \tag{4-3}$$

where the objective function $F(z)$ is a nonlinear function, A_L is an m_L, x n constant matrix of general linear constraints, and $c(x)$ is an m_N - vector of nonlinear constraint functions. the objective function F and the constraint functions are assumed to be smooth, i.e., at least twice-continuously differentiable. (The method of NPSOL will usually solve NP if there are only isolated discontinuities away from the solution).

Note that upper and lower bounds are specified for all the variables and for all the constraints. This form allows full generality in specifying other types of constraints. In particular, the *i-th* constraint may be defined as an equality by setting $\ell_i = u_i$. If certain bounds are not present, the associated elements of ℓ or u can be set to special values that will be treated as $-\infty$ or $+\infty$.

Here we briefly summarize the main features of the method of NZSOL and NPSOL as discussed in Reference 6 because Reference 12 is not available to general public. At a solution of NP, some of the constraints will be active, i.e., satisfied exactly. An active simple bound constraint implies that the corresponding variable is fixed at its bound, and hence the variables are partitioned into fixed and free variables. Let C denote the m x n matrix of gradients of the active general linear and nonlinear constraints. The number of fixed variables will be denoted by n_{FX}, with n_{FR} ($n_{FR} = n - n_{FX}$) the number of free variables. The subscripts *"FX"* and *"FR"* on a vector or matrix will denote the vector or matrix composed of the components corresponding to fixed or free variables. The details are discussed in Reference 11.

A point x is a first-order Kuhn-Tucker point for NP if the following conditions hold:

(i) x is feasible;
(ii) there exist vectors ζ and λ (the Lagrange multiplier vectors for the bound and general constraints) such that

$$g = C^T \lambda + \zeta, \tag{4-4a}$$

where g is the gradient of F evaluated at x, and $\zeta_j = 0$ if the *j-th* variable is free.

(iii) The Lagrange multiplier corresponding to an inequality constraint active at its lower bound must be non-negative, and non-positive for an inequality constraint active at its upper bound.

Let Z denote a matrix whose columns form a basis for the set of vectors orthogonal to the rows of C_{FR}; i.e., $C_{FR}Z = 0$. An equivalent statement of the condition in terms of Z is

$$Z^T g_{FR} = 0 \tag{4-4b}$$

The vector $Z^T g_{FR}$ is termed the projected gradient of F at x. Certain additional conditions must be satisfied in order for a first-order Kuhn-Tucker point to be a solution of NP.

4.1 The Quadratic Programming Subproblem

Similar to NPSOL, the basic structure of NZSOL involves major and minor iterations. The major iterations generate a sequence of iterates (x_k) that converge to x^*, a first-order Kuhn-Tucker point of NP. At a typical major iteration, the new iterate $\bar{x}$ is defined by

$$\bar{x} = x + \alpha p, \tag{4-5a}$$

where x is the current iterate, the non-negative scalar α is the step length, and p is the search direction. Also associated with each major iteration are estimates of the Lagrange multipliers and a prediction of the active set.

The search direction p is the solution of a quadratic programming subproblem of the form

$$\begin{aligned} &\underset{p}{\text{minimize}} && g^T p + \frac{1}{2} p^T H p \\ &\text{subject to} && \bar{\ell} \le \begin{Bmatrix} p \\ A_L p \\ A_N p \end{Bmatrix} \le \bar{u}, \end{aligned} \tag{4-5b}$$

where g is the gradient of F at x, the matrix H is a positive-definite quasi-Newton approximation to the Hessian of the Lagrangian function and A_N is the Jacobian matrix of c evaluated at x.

The estimated Lagrange multipliers at each major iteration are the Lagrange multipliers from the subproblem (and similarly for the predicted active set) and provide information about the the sensitivity of these NLP problems.

Certain matrices associated with the QP subproblem are relevant in the major iterations. Let the subscripts *"FX"* and *"FR"* refer to the predicted fixed and free variables, and let C denote the $m \times n$ matrix of gradients of the general linear and nonlinear constraints in the predicted active set. First, we have available the TQ factorization (Reference 11) of C_{FR} :

$$C_{FR}\, Q_{FR} = (0 \quad T), \tag{4-6}$$

where T is a nonsingular $m \times m$ reverse-triangular matrix (i.e., $t_{ij} = 0$ if $i + j < m$), and the non-singular $n_{FR} \times n_{FR}$ matrix Q_{FR} is the product of orthogonal transformations. Second, we have the upper-triangular Cholesky factor R of the transformed and re-ordered Hessian matrix

$$R^T R = H_Q \equiv Q^T \overline{H} Q, \tag{4-7}$$

where $\overline{H}$ is the Hessian H with rows and columns permuted so that the free variables are first, and Q is the $n \times n$ matrix

$$Q = \begin{pmatrix} Q_{FR} & \\ & I_{FX} \end{pmatrix}, \tag{4-8}$$

with I_{FX} the identity matrix of order n_{FX}. If the columns of Q_{FR} are partitioned so that

$$Q_{FR} = (Z \quad Y), \tag{4-9}$$

the n_Z $(n_Z \equiv n_{FR} - m)$ columns of Z form a basis for the null space of C_{FR}. The matrix Z is used to compute the projected gradient $Z^T g_{FR}$ at the current iterate.

As discussed in Reference 6 and 11, a theoretical characteristic of SQP methods is that the predicted active set from the QP subproblem is identical to the correct active set in a neighborhood of x^*. In NPSOL, this feature is exploited by using the QP active set from the previous iteration as a prediction of the active set for the next QP subproblem, which leads in practice to optimality of the subproblems in only one iteration as the solution is approached. Separate treatment of bound and linear constraints in NPSOL also saves computation in factorizing C_{FR} and H_Q.

4.2 The merit function

Detailed discussions of the merit function are given in Reference 14. In NZSOL and NPSOL, once the search direction p has been computed, the major iteration proceeds by determining a steplength α that produces a "sufficient decrease" in the augmented Lagrangian merit function

$$L(x,\lambda,s) = F(x) - \sum_i \lambda_i (c_i(x) - s_i) + \frac{1}{2} \sum_i \rho_i (c_i(x) - s_i)^2, \tag{4-10}$$

where x, λ and s vary during the line search. The summation terms involve only the nonlinear constraints. The vector λ is an estimate of the Lagrange multipliers for the nonlinear constraints of NP. The non-negative slack variable $\{s_i\}$ allow nonlinear inequality constraints to be treated without introducing discontinuities. The solution of the QP subproblem (4-5) provides a vector triple that serves as a direction of search for the three sets of variables.

4.3 The quasi-Newton updated

Before going into the detailed discussions, it is important to point out that both the NZSOL and NPSOL start by initializing the Hessian matrix H = Identity matrix. Thus at the beginning, the search direction is in the steepest decent direction. No initial curvature information is computed and the curvature information is accumulated through the BFGS quasi-Newton updates. The matrix H in (4-5) is a positive-definite quasi-Newton approximation to the Hessian of the Lagrangian function. At the end of each major iteration, a new Hessian approximation H is defined as a rank-two modification of H. In NPSOL the BFGS quasi-Newton update is used:

$$\bar{H} = H - \frac{1}{s^T H s} H s s^T H + \frac{1}{y^T s} y y^T, \tag{4-11}$$

where $s = \bar{x} - x$ (the change in x).

Rather than modifying H itself, the Cholesky factor of the transformed Hessian H_Q (4-7) is updated, where Q is the matrix from (4-8) associated with the active set of the QP subproblem. The update (4-11) is equivalent to the following update to H_Q :

$$\bar{H}_Q = H_Q - \frac{1}{s_Q^T H_Q s_Q} H_Q s_Q s_Q^T H_Q + \frac{1}{y_Q^T s_Q} y_Q y_Q^T, \tag{4-12}$$

where $y_Q = Q^T y$ and $s_Q = Q^T s$. This update may be expressed as a rank-one update to R and is used to incorporate new curvature information obtained in the move from x to $\bar{x}$.

4.4 NZSOL, NPSOL 4.02, and NPSOL 2.1

For those who are interested in applying these NLP codes, there are two publised versions of NPSOL. The NPSOL 4.02 was developed after the NPSOL 2.1 and therefore more reliable and efficient algorithm were incorporated according to Gill (Reference 12). However, in updating the Cholesky factor, the NPSOL 4.02 updates the whole or complete R while the NPSOL 2.1 updates only the part associated with the Z-space or null space of R. For the problem formulated here ,usually several hundred varibles are involved and the NPSOL 2.1 converges in less computing time. The NZSOL (Reference 12) incorporates not only latest efficient and reliable algorithm but also updates only the part of R associated with the null space of R only. In addition to improve the algorithm of NPSOL, it also adopts the best parts of both NPSOL 2.1 and 4.02.

Finally, it may be interesting to point out that the matrices in the present formulation using collocation and Hermite polynomial are large and fairly sparse. For computational efficiency, it is important to incorporate NLP codes such as MINOS (Reference 13) to take advantage of the special characteristic of the collocation formulation discussed here.

5. NUMERICAL RESULTS AND DATA

The data used in the numerical experiments presented here (c.f. Reference 2 and 9) are summarized as follows:

$$C_{DO} = 0.1 \quad ; \quad K = 1.111 \quad ; \quad m/S = 300 \text{ kg/m}^2 \tag{5-1}$$

and the drag polar is

$$C_D = C_{DO} + K * C_L^2 \qquad (5\text{-}2)$$

and other data are

$$\rho_a = 1.225\,kg/m^3;\ \mu = 3.986x10^{14}\,m^3/sec^2$$
$$\beta = 1/6900\,m^{-1};\ R_E = 6378\,km$$
$$H_a = 120\,km;\ R_d = 12996\,km;\ R_c = 6558\,km \qquad (5\text{-}3)$$

Using the above mentioned data, simulations were carried out. The optimal solution for the reference case (shown in figures as Case 1) has the following entry and exit status.

Entry status: $H_e = 120$ km; $V_e = 9034.74$ m/sec
$\gamma_e = -4.36$ degrees; $\phi_e = 0$; $\psi_e = 0$ (5-4)

Exit status: $H_f = 120$ km; $V_f = 7028.95$ m/sec
$\gamma_f = 0.0$ deg; $\phi_f = -6.69$ deg
$\psi_f = 18.891$ deg; total flight time = 478 sec (5-5)

Characteristic velocities:

Deorbit characteristic velocity	$\Delta V_d = 1031.59$ m/sec
Boost characteristic velocity	$\Delta V_b = 821.49$ m/sec
Reorbit characteristic velocity	$\Delta V_c = 17.98$ m/sec
Total characteristic velocity	$\Delta V = 1871.07$ m/sec (5-6)

Time histories of altitude, velocity, flight path angles, heading angles, dynamical pressure, atmospheric density, orbit inclination and heating rate are shown in Figure 3-10. Figures 11-13 show lift coefficient, bank angle, and lift to drag ratio as a function time for several simulation runs for the reference case(.i.e., Case 1). These simulation runs show that at high altitude the control may be different for different simulation runs depending upon initial guesses. This is really not a surprise because at high altitude, the aerodynamic forces or the controls are ineffective. In fact, the problem has a weak optimium with respect to the controls at high altitude.

Without going into the details, the characteristic velocities for the cases with orbital inclination changes for 15, 20 and 25 degrees are summarized in Table 2.

The heating rate Q_r , along the atmospheric trajectory, is computed for the stagnation point of a sphere of radius of one meter, according to the following relation (Reference 2 and 6)

$$Q_r = K_r \rho^{0.5} V^{3.08} \qquad (5\text{-}7)$$

where the ρ is the atmospheric density in kg/km^3, V is the velocity in km/sec and the K_r is the proportionality constant equal to 0.000308. The peak heating rate for the reference case is about 239 W/cm^2. Simulation results for cases with peak heat rate constrained to 203 W/cm^2 and 170 W/cm^2 were also obtained and shown in Figures 3-10 in comparison with the reference case without heat constraints as Case 2 and 3 respectively. These two cases reduces the peaking heating rate of the reference case by 15 and 30 percent respectively. Simulation results presented here provide the sensitivity of trajectory and associated physical variables as the heating constraints are imposed.

Similarly, the characteristic velocities for the cases with heating constraints are summarized in Table 2. The percent reductions are with respect to the peak heating rate of the reference case without heat constraints. As shown here, one needs less thermal protection materials and more fuel consumption to fly the heat constrained trajectories and therefore by taking into account the weight of thermal protection materials one may find an optimal design to minimize the total vehicle weight.

Another interesting observation from the data given in Table 1 and 2 is that the deorbit impulse is almost the same for all the cases simulated here. The total characteristic velocity for a given optimal trajectory is almost completely determined by the boost and the recirculation. In fact, the boost velocity contributes the most to the variation of the total characteristic velocity. Physically, it is obvious as the vehicle makes a larger turn it also loses more energy and therefore needs more velocity to boost it back to the final orbital altitude. Although the total characteristic velocity is insentive to the magnitude of deorbit impulse, the optimal trajectory is very sensitive to ΔV_d.

6. CONCLUDING REMARKS

An excellent survey of the subject was given in Reference 1. Walberg reviewed the problem of synergetic plane change for optimal orbital transfer. In a recent paper by Naidu (c.f. Reference 2), fuel optimal trajectories of aeroassisted orbital transfer with plane change were presented using the so-called multiple shooting method for the case without heat constraints and under the assumption that all the synergetic plane change was performed entirely in the atmosphere. A brief review of the progress made in this field was also given in Reference 2. In our paper, a similar problem for cases with and without stagnation point heating rate constraints was solved using the collocation and nonlinear programming technique. This method is especially suitable for parametrical studies because of its relative insensitivity to initial guesses. Once a solution for a reference case is obtained, solutions for other cases such as different orbital inclination change can be obtained easily.

Finally, the present problem can also be formulated under a more general assumption that not all the plane changes are entirely made in the atmosphere. It must be noted that the AOTV transfer can be made more efficient propulsively if the plane change is performed partly in the atmosphere and partly in space and the propulsive plane change in space is subdivided into components associated with various impulsive points. For the more general formulation discussed, the desired plane change may consist of more than one plane change, i.e.

$$\text{Total orbital plane change} = i_1 + i_2 + i_3 + i_a$$

where i_1, i_2, and i_3 are plane changes at the deorbit, reboost, and reorbit respectively and i_a is the aeroassisted plane change and all these plane changes will be determined by the optimization processes discussed here. Preliminary simulation results were obtained and are to be published in the near future.

It should be mentioned that the collocation and nonlinear programming technique discussed here was recently applied to another group of orbital transfer problem by Enright and Conway in Reference 3 and the relative insensitivity of this method to the initial guesses was also observed by them. Our basic simulation test bed is the OTIS codes (Reference 5) with an improved and updated nonlinear programming code (NZSOL). All physical models used were documented in Reference 5. Of course, necessary modifications and corrections have to be incorporated to simulate the aerobraking problems discussed here.

It may be worthwhile mentioning that the present problem was actually solved by guessing the initial state and control varibles at four selected points , i.e., the initial point, the final point and two other nodal points along the trajectory inside the atmosphere. The initial state and control variables at other nodes or grid points were simply obtained by linear interpolation. These initial guesses do not have to satisfy either the governing equations or the nonlinear constriants including the defects. Only roughly guesses are needed at these four points. Converged solutions were obtained with relative ease. However, it is important to point out proper scaling of the defects, constraints and variables are essential to get converged solutions. Although our results were compared with the draft paper of Reference 2, the solution presented by Naidu was not actually optimal because the final flight path angle $\gamma_f = -0.6217$ degrees is negative. For simulations discussed here, converged solutions were obtained by using as little as 20 nodes. However, in some cases, converged solutions were obtained using 60 nodes, In the later case, the problem has more than 660 independent variables and more than 400 nonlinear "defects" equations. For cases with heating rate constraints, the problem has more than 500 nonlinear constraint equations includinding the "defect" equations. As far as we know, this may be the first time converged soultions were obtained for so many independent variables and nonlinear constraint equations. This also illustrates how powerful the nonlinear programming code and the collocation and Hermite polynomial technique are.

Finally, it is important to mention again that aeroassisted orbital transfer introduces a strong coupling between the vehicle design and the trajectory design as indicated by the simulation data. A trajectory that minimizes fuel mass, without attention to heating , may require the vehicle to have a heavy thermal protection systems. As shown here, an optimal design for the total vehicle weight may be obtained as discussed earlier. However, if the aeroassisted transfer is to be prefered to all propulsive transfer, it must offer a reduction in fuel mass greater than the increase in thermal protection mass.

7. REFERENCES

1. Walberg, G. A., "A Survey of Aeroassisted Orbit Transfer", Journal of Spacecraft and Rockets, Vol. 22, Jan-Feb. 1985, pp 3-18.

2. Naidu, D. S., "Fuel-optimal Trajectories of Aeroassisted Orbital Transfer with Plan Change" AIAA Guidance, Navigation & Control Conference, Boston, MA., August 14-16, 1989.

3. Enright, P. J. and Conway, B. A., "Optimal Finite Thrust Spacecraft Trajectories Using Collocation and Nonlinear Programming", Paper AAS 89-350, AAS/AIAA Astrodynamics Specialist Conference, Stowe, Vermont, August 7-10, 1989.

4. Shi, Y. Y.," Matched Asymptotic Solution For Optimum Lift Controlled Atmospheric Entry ", AIAA JOURNAL, VOL. 9, 1971, PP. 2229-2238.

5. Hardgraves, C. R.and Paris, S. W., " OTIS-Optimal Trajectories by Implicit Integration ", Boeing Aerospace Co., Contract No. F33615-85-C-3009,1988.

6. Gill, P.E., Murray, W., Sanders, M.A., and Wright, M.H., " User's Guide For NPSOL (Version 4.0) : A Fortran Package For Nonlinear Programming ", System Optimization Laboratory, Department of Operation Research, Standford University, Stanford, Claifornia, 1986.

7. Shi, Y. Y., Pottsepp, L., and M. C. Eckstein. " Optimal lift Control of a Hypersonic Lifting Body During Atmospheric Entry ", AIAA Journal, Vol.7, No.12, December,1969..

8. Shi, Y. Y. and Eckstein, M. C., "An Exact Solution for Optimum Controlled Soft Lunar Landing", Astronautica Acta, Vol.16, pp. 9-18, Pergamon Press, New York, 1971.

9. Mease,K.D.and Vinh, N. X.," Minimum-Fuel Aeroassisted Coplanar Orbit Transfer Using Lift-Modulation', AIAA Journal of Guidance and Control, Vol.8,No.1, Jan-Feb. 1985.

10. Mease,K.D., "Optimization of Aeroassisted Orbital Transfer : Current Status", The Journal of the Astronautical Sciences, Special Issue On Hypervelocity Flight,Volume 36, Nos.1/2, January-June,1988.

11. Gill, P.E., and Wright, M.H., " Practical Optimization ", Academic press, London and New York, 1981.

12. Gill, P.E.," NZSOL: An Improved Version of NPSOL", Private Communications , Huntington Beach, California,1989-90.

13. Murtagh, B. A. and Saunders, M.A., " MINORS 5.0 User's Guide", Report SOL 83-20, Department of Operation Research, Standford Research, California, 1983.

14. Gill, P.E., Murray, W., Sanders, M.A., and Wright, M.H.," Some Theoretical Properties of An Augmented Lagragian Merit Function ", Technical Report SOL 86-6R, System Optimization Laboratory, Department of Operation Research, Standford University, Stanford, Claifornia, 1986.

TABLE 1

EFFECTS OF HEAT CONSTRANTS ON CHARACTERISTIC VELOCITIES

PEAK HEATING RATES	ΔV_1	ΔV_2	ΔV_3	TOTAL
(WATTS/cm)	(m/sec)	(m/sec)	(m/sec)	(m/sec)
UNCONSTRAINED $\dot{Q}$ = 239	1031	821	18	1870
DR. NAIDU (BNDSCO) UNCONSTRAINED	1034	816	43	1893
HEAT CONSTRAINT $\dot{Q}$ = 203	1028	855	18	1901
HEAT CONSTRAINT $\dot{Q}$ = 170	1026	930	19	1974

TABLE 2

CHARACTERISTIC VELOCITIES FOR DIFFERENT ORBIT INCLINATION CHANGES

Δi	ΔV_1	ΔV_2	ΔV_3	TOTAL ΔV
(degree)	(m/sec)	(m/sec)	(m/sec)	(m/sec)
15	1029	312	21	1362
20	1031	821	18	1871
25	1035	1270	31	2336

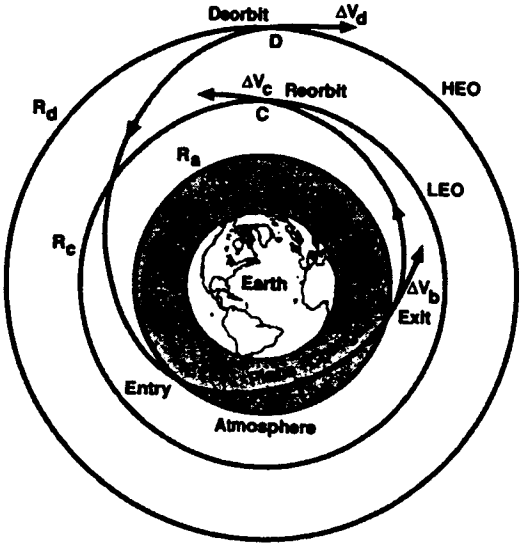

Fig. 1 Aeroassisted Orbital Plane Change

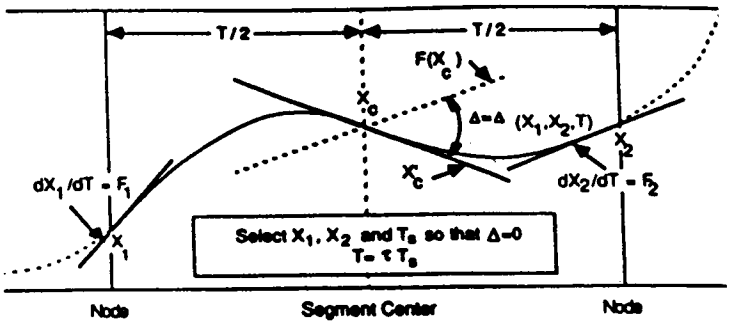

Fig. 2 Collocation and Hermite Approximation

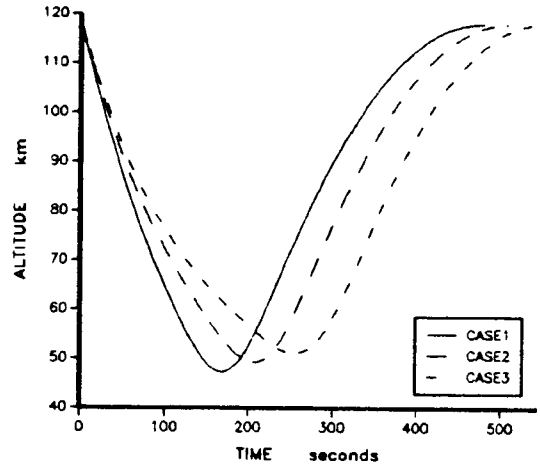

Fig.3 Time History of Altitude

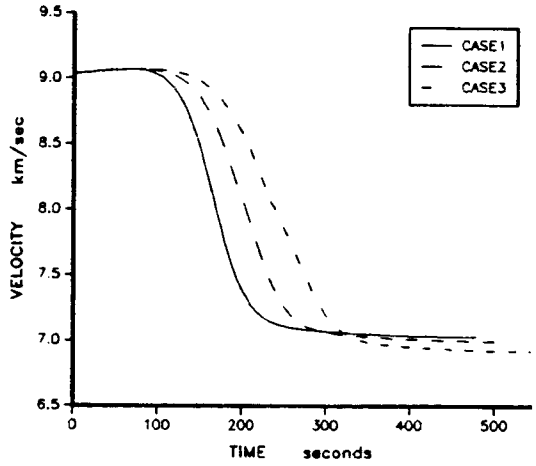

Fig.4 Time History of Velocity

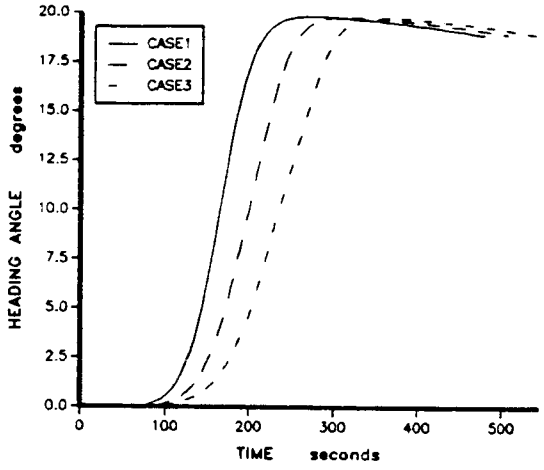

Fig.5 Time History of Heading Angle

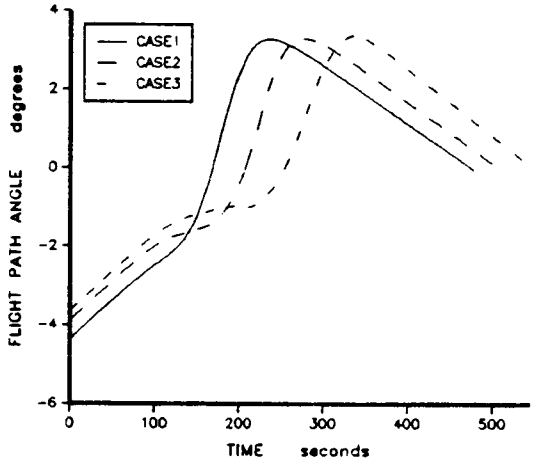

Fig.6 Time History of Flight Path Angle

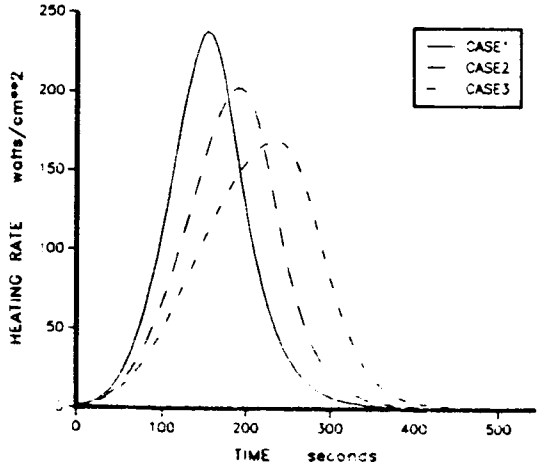

Fig.7 Time History of Heating Rate

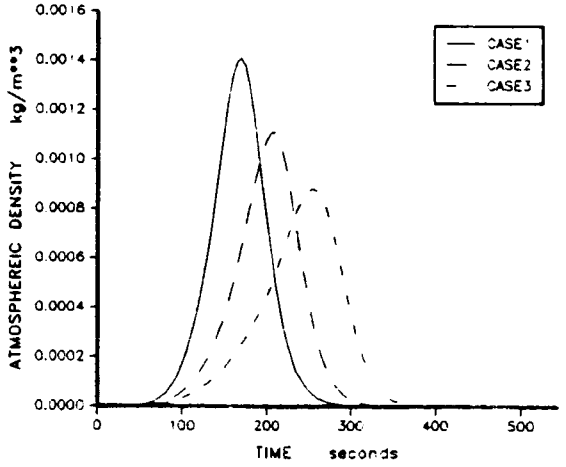

Fig.8 Time History of Atmospheric Density

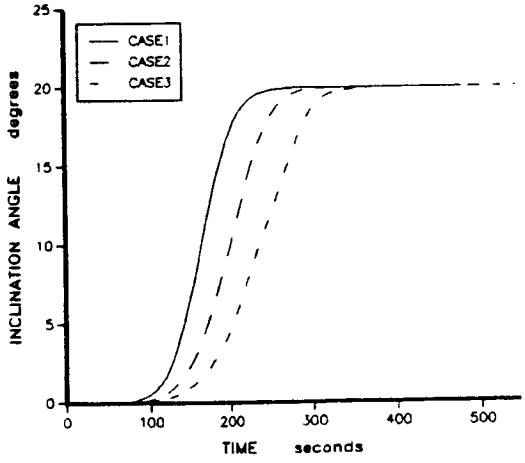

Fig.9 Time History of Inclination Angle

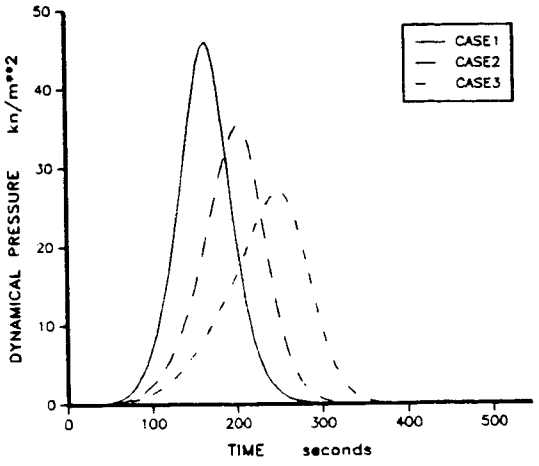

Fig.10 Time History of Dynamical Pressure

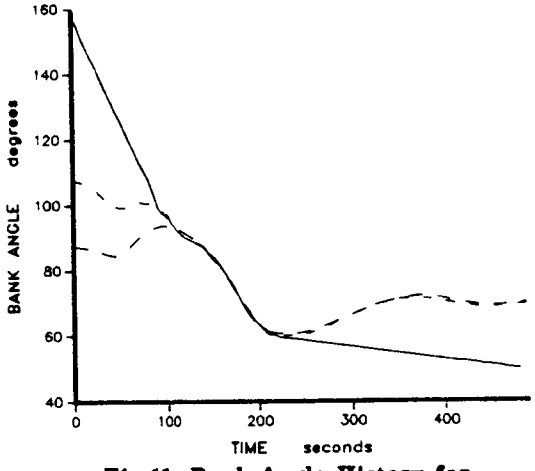

Fig.11 Bank Angle History for Reference Case

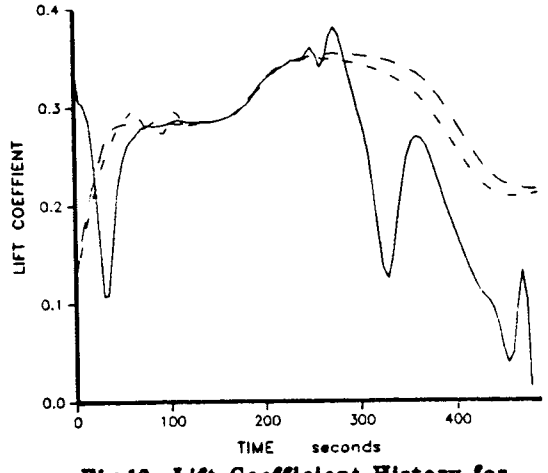

Fig.12 Lift Coefficient History for Reference Case

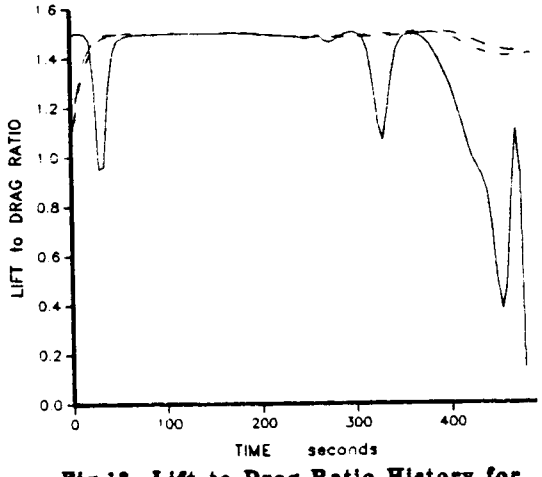

Fig.13 Lift to Drag Ratio History for Reference Case